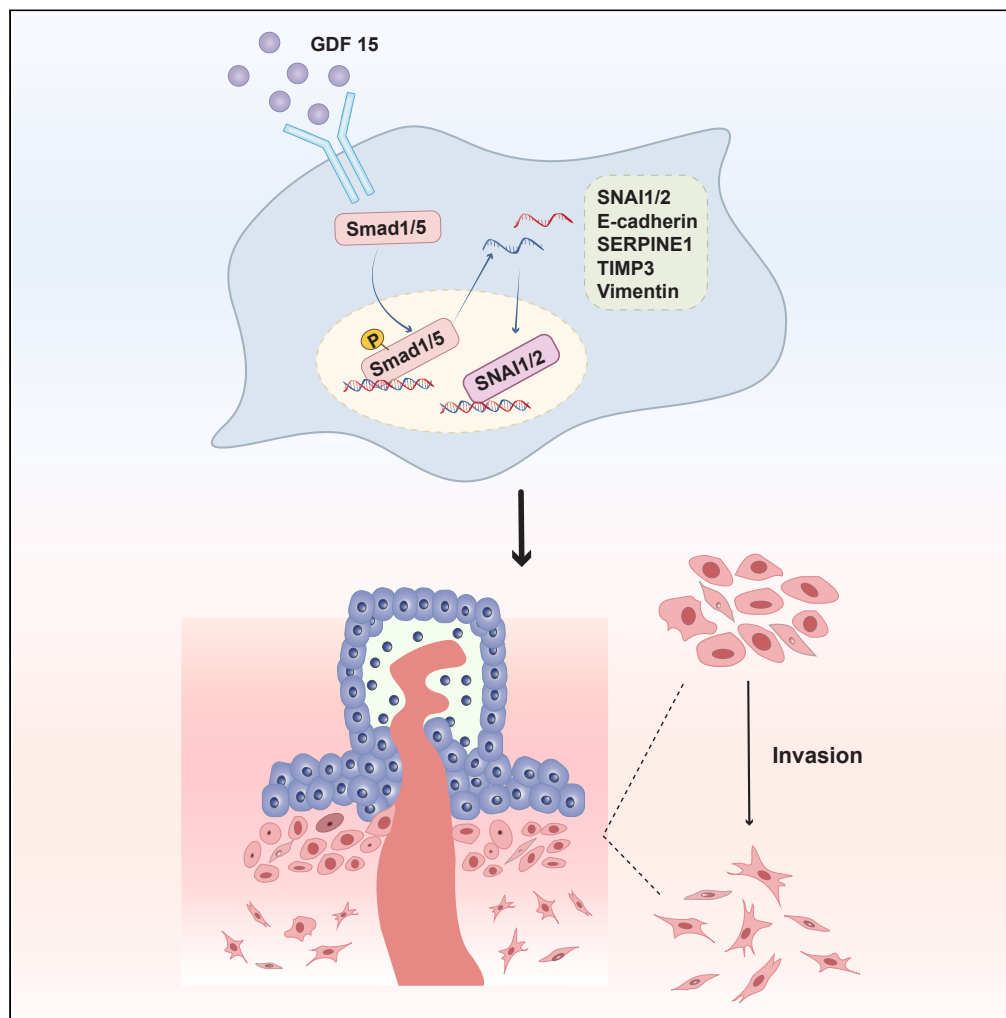


Article

GDF15 deficiency hinders human trophoblast invasion to mediate pregnancy loss through downregulating Smad1/5 phosphorylation



Yu-Ting Zeng,
Wen-Fang Liu,
Peng-Sheng
Zheng, Shan Li

zpsheg@mail.xjtu.edu.cn (P.-
S.Z.)
lishan2.0521@stu.xjtu.edu.cn
(S.L.)

Highlights

Trophoblastic cells
produce GDF15 which
works through autocrine
and paracrine modes

GDF15 phosphorylates
Smad1/5 in trophoblast
cells through binding to its
receptor

Phosphorylated Smad1/5
activates target genes,
such as SNAI1/2,
E-Cadherin, Vimentin

Article

GDF15 deficiency hinders human trophoblast invasion to mediate pregnancy loss through downregulating Smad1/5 phosphorylation

Yu-Ting Zeng,¹ Wen-Fang Liu,¹ Peng-Sheng Zheng,^{1,2,*} and Shan Li^{1,3,*}

SUMMARY

Growth differentiation factor 15 (GDF15) belongs to the Transforming growth factor β (TGF- β) superfamily. The decrease of GDF15 in the serum of pregnant women was associated with miscarriage. Both IHC and ELISA assays showed that GDF15 in trophoblast tissue and serum of pregnant women who miscarried was significantly lower than in those who had a live birth. GDF15 deficiency was associated with embryo resorption in GDF15 knockout mice through CRISPR editing. In addition, the migration and invasion ability of HTR-8/SVneo and JEG-3 cells were promoted by GDF15. Mechanistically, GDF15 increased Smad1/5 phosphorylation, resulting in upregulating SNAI1/2, VIMENTIN and downregulating E-CADHERIN. A dual-luciferase reporter assay confirmed that Smad-binding elements (SBE) and/or GC-rich motifs were activated and target genes such as SNAI1/2, SERPINE1, and TIMP3 were transcriptionally regulated by GDF15/Smad5 signaling. Therefore, our data revealed a crucial role of GDF15 on invasion of trophoblast by upregulating the activity of TGF- β /Smad1/5 pathway.

INTRODUCTION

The developing of trophoblast cells from implanting blastocyst is the key event in the establishment of pregnancy.¹ Miscarriage usually refers spontaneous pregnancy loss which involves many pathological events including disorder of placentation. TGF- β s, GDFs, BMPs, activins, inhibitors, and anti-Mullerian hormone (AMH) belong to the transforming growth factor (TGF- β) family. The TGF- β superfamily members exert divergent functions in regulating extravillous trophoblasts (EVTs) invasion, which contribute to the balance of maternal-fetal interface during the pregnancy.² TGF- β 1 was proved to inhibit trophoblast cell invasion by inducing Snail-mediated downregulation of VE-cadherin.³ GDF8 promotes trophoblast cell invasion by inducing ALK5-SMAD2/3-mediated MMP2 upregulation.⁴ GDF11 stimulates trophoblast cell invasion by upregulated ID2/MMP2 pathway signaling.⁵ BMP2 promotes human trophoblast cell invasion and endothelial-like tube formation through ID1-regulated IGFBP3 expression.⁶ However, the mechanism of GDF15 in trophoblast cells invasion is not completely understood.

GDF15 is widely distributed in mammal and plays many pivotal roles in the physiological status such as pregnancy, inflammation, cancer, cardiovascular disease and obesity.⁷ GDF15 is detected in the sera of pregnant women and the level rises substantially with progress of gestation trimester. GDF15 can also be detected both in amniotic fluid and placental extracts in high levels. According to these findings, the placental trophoblast is a major source of the GDF15 present in maternal serum and amniotic fluid.^{8,9}

In the present study, we examine the expression of GDF15 in the trophoblast tissues and cells as well as its involvement in the pro-invasive effects on HTR-8/SVneo and JEG-3 cell lines. The decrease of GDF15 level in villus indicated the disorder of trophoblast invasion and a risk of miscarriage. Our results indicated that GDF15 induced the phosphorylation of Smad1/5, which subsequently *trans*-regulated target genes such as SNAI1/2, SERPINE1 and TIMP3 which promoted the invasion of trophoblast cells.

RESULTS

GDF15 expression in trophoblast and serum of pregnant women with and without miscarriage

To explore the role of GDF15 in the trophoblast and serum of pregnant women, GDF15 protein expression was detected in the villus from curettage of women without medical reasons (Normal, N = 18) and women with spontaneous miscarriage (Miscarriage, N = 16) samples using immunohistochemistry (Figure 1A). The immunoreactivity score (IRS) of GDF15 staining decreased from 8.22 ± 0.76 in normal samples to 4.31 ± 0.37 in miscarriage samples (Figure 1B, $p < 0.001$). Moreover, GDF15 staining was graded into three categories: negative, weakly positive and strongly positive. Negative GDF15 staining was found in 0.00% of normal tissue (0/18) and 18.8% in miscarriage tissue (3/16). Weak positive GDF15 staining was found in 27.8% of normal tissue (5/18) and 68.8% of miscarriage tissue (11/16). The percentage of strong positive

¹Department of Reproductive Medicine, The First Affiliated Hospital of Xi'an Jiaotong University, Xi'an, Shaanxi, China²Key Laboratory of Environment and Genes Related to Diseases, Ministry of Education of the People's Republic of China, Xi'an, Shaanxi, China³Lead contact

*Correspondence: zpszheng@mail.xjtu.edu.cn (P.-S.Z.), lishan2.0521@stu.xjtu.edu.cn (S.L.)

<https://doi.org/10.1016/j.isci.2023.107902>

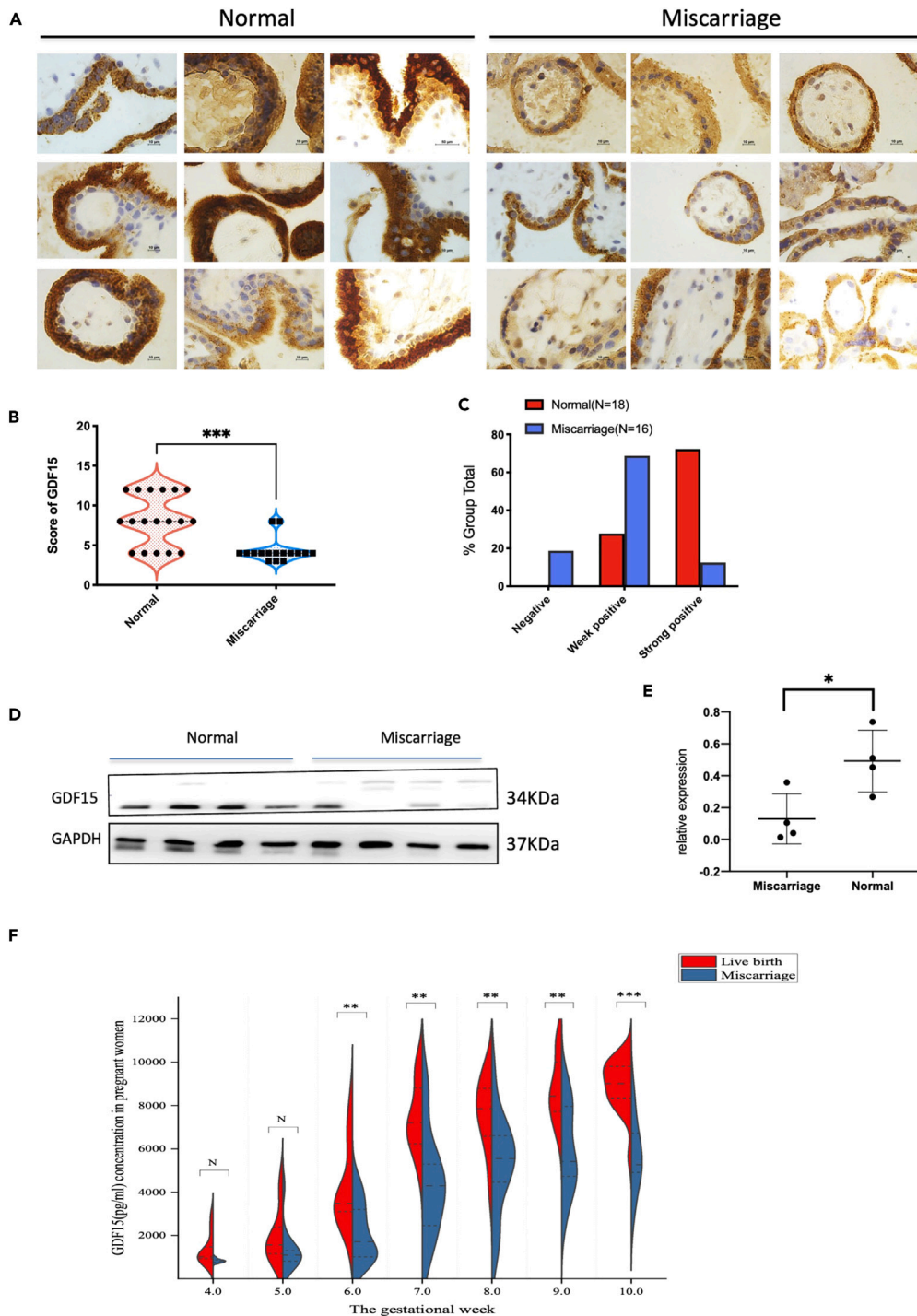


Figure 1. Expression of GDF15 in trophoblast tissues and serum of pregnant women

(A) Immunohistochemical (IHC) detection of GDF15 in the villus from curettage of women without medical reasons (Normal) and women with spontaneous miscarriage (Miscarriage) samples; original magnification, 400x.

(B) The scatterplot presents the immunoreactivity scores obtained for GDF15 staining in Normal and Miscarriage samples.

(C) The bar chart illustrates the percentage of negative, week positive and strong positive groups classified by GDF15 staining.

(D and E) (D) The expression of GDF15 in the normal and miscarriage villus samples was detected by western blotting and the quantitative analysis were shown (E).

(F) The serum concentrations of GDF15 in the pregnant women during 4–10 weeks with miscarriage and with live birth were detected by ELISA. Data were presented as Violin diagram. *, $p < 0.05$; **, $p < 0.01$; ***, $p < 0.001$ (unpaired two-tailed Student's t test). See also [Table S1](#) for further information.

GDF15 staining in normal tissue (13/18) was 72.2% while it was 12.5% in miscarriage tissue (2/16). The rate of positive GDF15 staining in normal tissue was significantly higher than that in miscarriage tissue (Figure 1C, $p < 0.05$). Consequently, GDF15 expression was detected by western blotting in four normal samples and four miscarriage samples, the expression of GDF15 relative to GAPDH was significantly lower in miscarriage than in normal samples (Figures 1D and 1E, $p < 0.05$). Furthermore, we randomly collected serum from pregnant women with a history of recurrent pregnancy loss during 4–10 gestational weeks. 36 serums from 15 patients who had a live birth while 40 serums from 20 patients who experienced miscarriage again in the follow-up. The levels of GDF15 in women with live births and with miscarriages were measured using ELISA and were shown in Table S1. GDF15 concentrates in the serum of women who had live births were much higher than those who had miscarriage, especially during 6–10 weeks (Figure 1F). The results of identification of trophoblastic cells and tissues using CK7 and HLA-G as markers are presented in Figures S1A–S1C. Immunocytochemical assays and Western blot analyses in trophoblast cells revealed that GDF15 was abundant in the HTR-8/SVneo, JAR and JEG-3 cell lines (Figures S1D–S1F). The overexpression and knockdown efficiency of GDF15 was shown in the HTR-8/SVneo and JEG-3 cell lines (Figures S1G and S1H).

The single-cell RNA-seq analysis of GDF15 expression in The Human Cell Landscape (HCL) database

We analyzed GDF15 expression in The Human Cell Landscape (HCL) database using single-cell RNA-seq (bis.zju.edu.cn/HCL/). Over 700,000 single cells from more than 50 human tissue were classified into 102 major clusters in the HCL database. The Landscape provides global view on single cell level (Figure S2A) and placental tissue clusters were highlighted (Figure S2B). In the Gallery, GDF15 was selected from single-cell digital gene expression matrix and the results of clustering analysis were displayed in Figure S2C. Sorting by GDF15 expression in clusters and tissues, GDF15 was found to be abundantly expressed in the prostate, kidney, placenta tissues (Figures S2D and S2E). Consistent results of scRNA-seq analysis from three different placental origins revealed that GDF15 was specifically found in extravillous trophoblast and syncytiotrophoblast cells (Figures S2F and S2G: Placenta1; Figures S2H and S2I: Placenta_Tsang; Figures S1J and S1K: Placenta_VentoTormo).

A decreased in GDF15 levels contributes to fetal loss in mice *in vivo*

Six placentas from pregnant mice with and without absorbed fetus were collected randomly using the abortion mouse model (CBA/J♀ × DBA/2♂, Figures 2A and 2B). GDF15 expression in the trophoblasts from mouse placenta was detected by immunochemistry (Figures 2C and 2D). In comparison to the trophoblast with a normal fetus, the trophoblast with an absorbed fetus had a considerably lower GDF15 staining score (Figure 2E). GDF15 transgenic mice (wild type: GDF15^{+/+}, heterozygote type: GDF15^{+/-}, homozygote type: GDF15^{-/-}) were used to assess the impact of GDF15 on embryo survival. 31 offspring with wild type, 62 with heterozygote type and 20 with homozygote type were born from 16 heterozygote pregnant mice (GDF15^{+/-}♀ × GDF15^{+/-}♂) included. The expected and observed actual distribution of offspring gene types are shown in Figure 2F. In order to compare fertility, three groups were made: wild type group (GDF15^{+/+}♀ × GDF15^{+/+}♂), heterozygote group (GDF15^{+/-}♀ × GDF15^{+/-}♂) and homozygote group (GDF15^{-/-}♀ × GDF15^{-/-}♂). All female mice were housed with male mice for 15 days in each group. The distribution of fertile and infertile female mice was depicted in Figure 2G. Both homozygote and heterozygote groups had higher rates of infertility than the wild type group ($p = 0.0427$). The period between cohabitation and delivery was not significantly different between the three groups (Figure 2H). Notably, the embryo resorption rate in the homozygote group was remarkably higher than that of the heterozygote and wild type groups (Figure 2I). The findings indicated that GDF15 deficiency contributed to embryo resorption and fetal loss in mice.

GDF15 promotes the migration and invasion of human trophoblast cells *in vitro*

A Transwell assay and a wounding-healing assay were applied to determine the effect of GDF15 on the motility of HTR8/Svneo and JEG-3 cells *in vitro*. After 48 h of incubation in a Transwell assay, the numbers of HTR8-shGDF15 and JEG-3-shGDF15 cells invading across the Matrigel-coated membrane were significantly lower than those of HTR8-shCON and JEG-3-shCON respectively. Recombinant GDF15 protein (HTR8-shGDF15+rhGDF15 and JEG-3-shGDF15+rhGDF15) added to the cells rescued this decrease in invasion (Figures 3A–3D, $p < 0.001$). Furthermore, the effect of GDF15 on the migratory capability of HTR8 and JEG-3 cells was detected in a Transwell migratory assay by uncoated inserts. The number of HTR8-shGDF15 and JEG-3-shGDF15 cells migrating across the uncoated membrane was markedly lower than that of HTR8-shCON and JEG-3-shCON cells respectively. Consistently, the addition of rhGDF15 (HTR8-shGDF15+rhGDF15 and JEG-3-shGDF15+rhGDF15) to cells reversed this decrease in migration (Figures 3A–3D, $p < 0.001$). Similarly, in the wounding-healing assay, HTR8-shGDF15 and JEG-3-shGDF15 cells significantly decreased wound closure compared to HTR8-shCON and JEG-3-shCON cells after 48 h, while the decrease in wound closure was rescued with rhGDF15 in HTR8-shGDF15+rhGDF15 and JEG-3-shGDF15+rhGDF15 cells (Figures 3E and 3F, $p < 0.05$). All of these results showed that GDF15 attenuation reduces the capacities of HTR8 and JEG-3 cells to invade and migrate *in vitro*.

GDF15 activates the TGF- β pathway and regulates epithelial-mesenchymal transition (EMT)-related genes in HTR8/SVneo cells

A transcriptome sequencing analysis of HTR8-shGDF15 and HTR8-shCon cell lines was performed to investigate the mechanism by which GDF15 promotes the motility of trophoblast cells. The differential expression genes including up-regulation and down-regulation were depicted as volcano map (Figure 4A). Kyoto Encyclopedia of Genes and Genomes (KEGG) pathway enrichment analysis suggested that

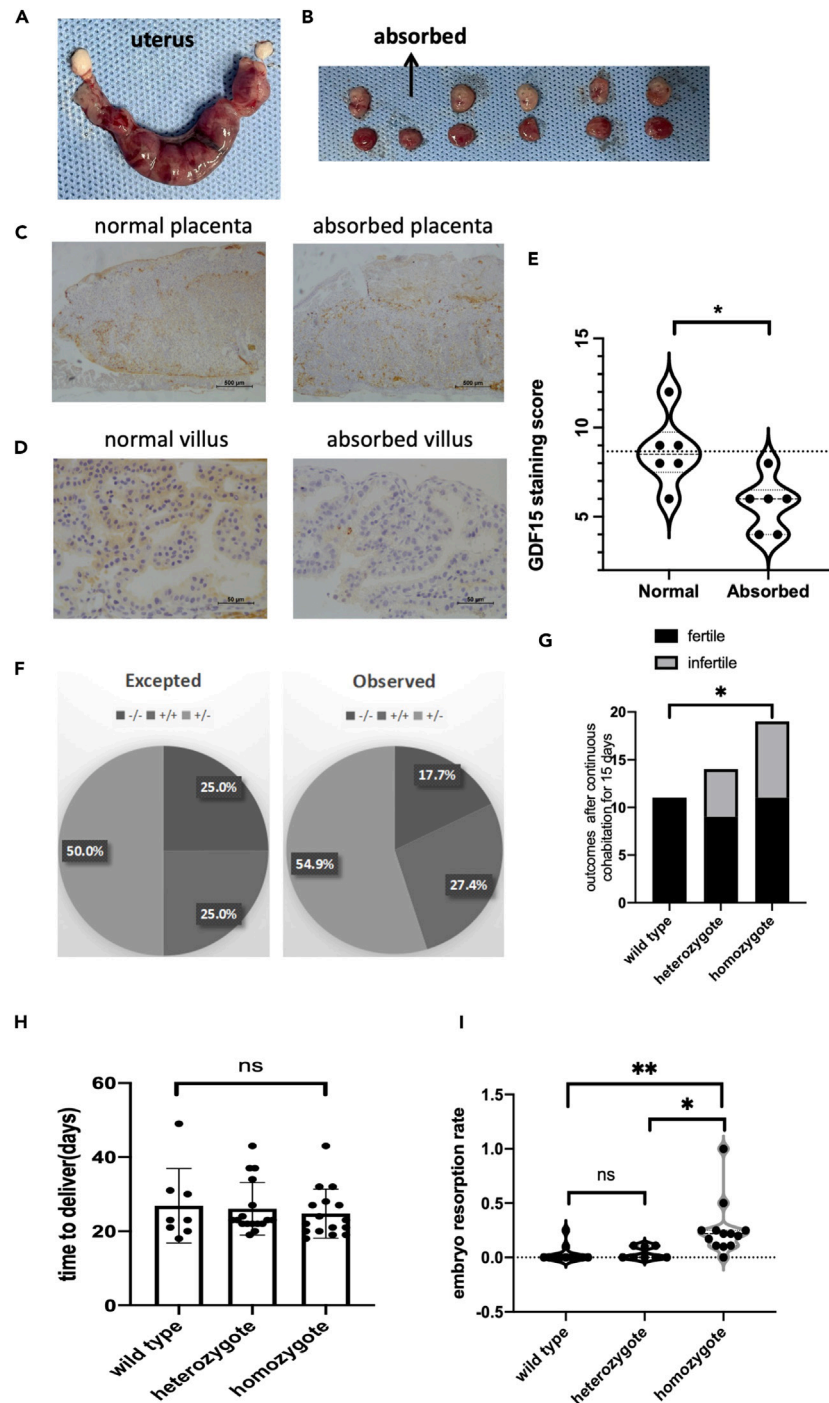


Figure 2. The decreased level of GDF15 participates in the process of fetal loss in mice *in vivo*

(A and B) (A) The uterus and placentas (B) with normal and absorbed fetus from pregnant CBA mice.

(C and D) (C) Immunohistochemical staining for GDF15 are shown in the placentas and villus (D) with normal and absorbed fetus.

(E) The quantitative analysis of GDF15 staining is shown in the violin plot.

(F) The pie chart presents the expected and observed percentages of genotypes of C57 transgenic mice offspring from heterozygous parents (GDF15 KO +/-); wild type: +/+, heterozygote: +/-; homozygote: -/-.

(G) The bar chart illustrates the percentage of fertile and infertile mice in the three genotype groups after continuous cohabitation for 15 days.

(H and I) (H) The time to deliver and embryo resorption rate at day 12.5 (I) in the three genotype groups. *, $p < 0.05$; **, $p < 0.01$; ***, $p < 0.001$ (unpaired two-tailed Student's *t* test).

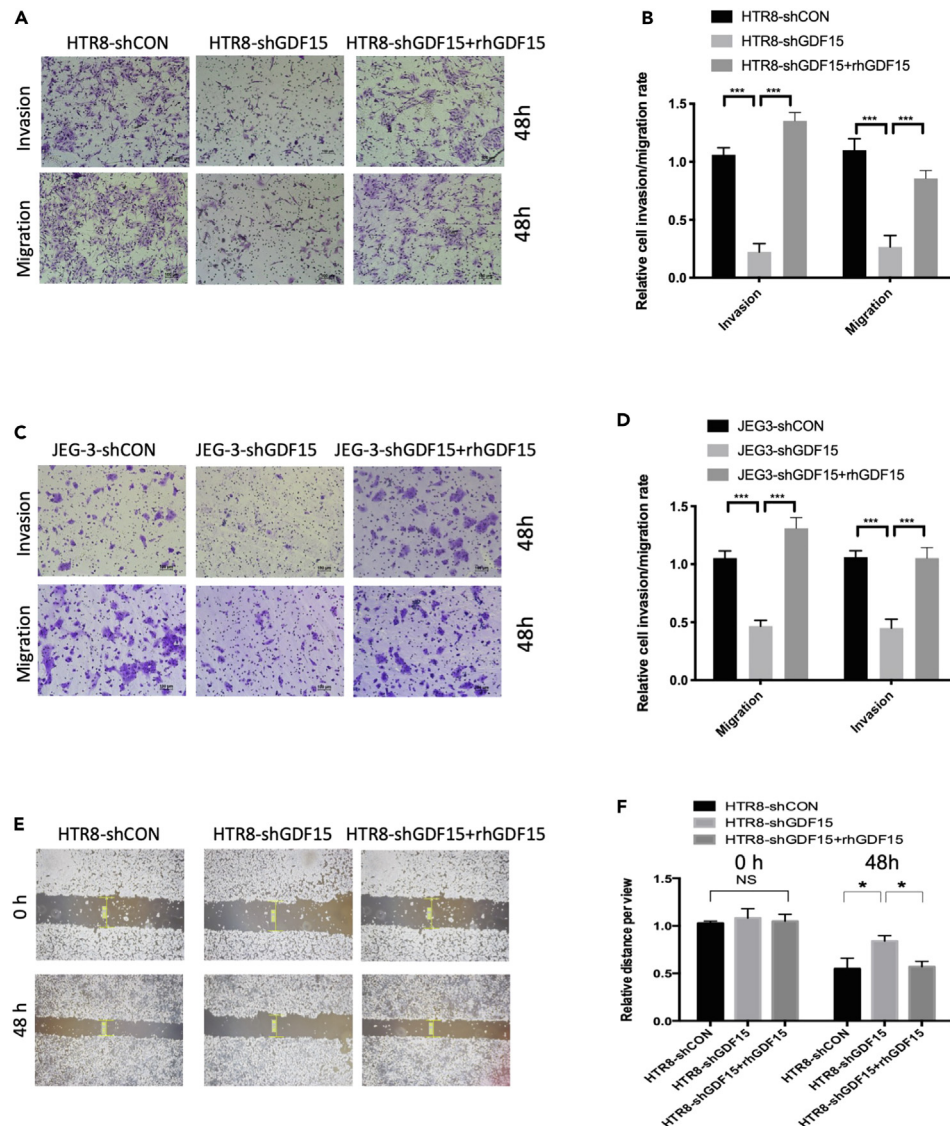


Figure 3. GDF15 promotes the migration and invasion of human trophoblast cells *in vitro*

(A and C) (A) The invasive and migratory potential of HTR8/Svneo and JEG-3(C) cells after silencing GDF15 and rhGDF15 rescue.

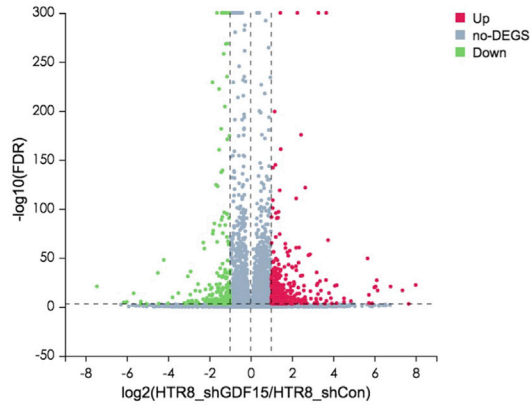
(B and D) (B) Numbers of invasive and migratory (D) cells were shown as mean \pm SD using triplicate measurements.

(E) The migratory potential of HTR8/Svneo cells after silencing and rhGDF15 rescue was analyzed in a wound-healing assay for 0 and 48 h.

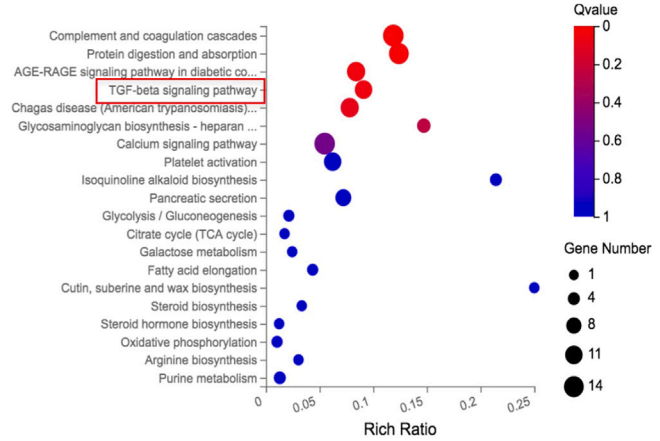
(F) Scratch area was shown as mean \pm SD using triplicate measurements. *, $p < 0.05$; **, $p < 0.01$; ***, $p < 0.001$ (unpaired two-tailed Student's *t* test).

TGF- β signaling pathway involved in the mechanism of GDF15 in trophoblast cells (Figure 4B). The expression of 15 genes regulated by TGF- β signaling pathway such as SERPINE1, TIMP3, ID1 and ID4 significantly differed between HTR8-shCon and HTR8-shGDF15 cells (Figure 4C). Gene Ontology (GO) enrichment analysis identified 13 epithelial-mesenchymal transition (EMT)-related genes, including SNAI1/2, MMP1, VIMENTIN and E-CADHERIN which exhibit the capacity of extracellular matrix, cell adhesion, cell migration, cell invasion, and whose expression remarkably differed between the two groups (Figure 4D). Furthermore, eight EMT-related genes and nine TGF- β signaling pathway-related genes were chosen for validation via real-time PCR assay. The mRNA of CDH1 (E-CADHERIN) was significantly increased, while levels of SNAI1/2, Vimentin, ZEB1, MMP1 and MMP2 were significantly decreased in the HTR8-shGDF15 compared to those in the control cells. The mRNA of ZEB2 was not altered in the two groups (Figure 4E, $p < 0.05$). In addition, the mRNA of SERPINE1, TIMP3, TGM2, PMEPA1, HMGA1 and IGFBP5 were significantly lower in the HTR8-shGDF15 compared to those in the control cells, whereas the mRNA of LTBP1 and LTBP2 were not altered in the two groups (Figure 4F, $p < 0.05$). β -actin was used as a reference gene in the above real-time PCR assay and related primers were listed in Table S2. All these findings indicated that GDF15 participated the migration and invasion of trophoblast cells, possibly by regulating the TGF- β signaling pathway and EMT-related genes.

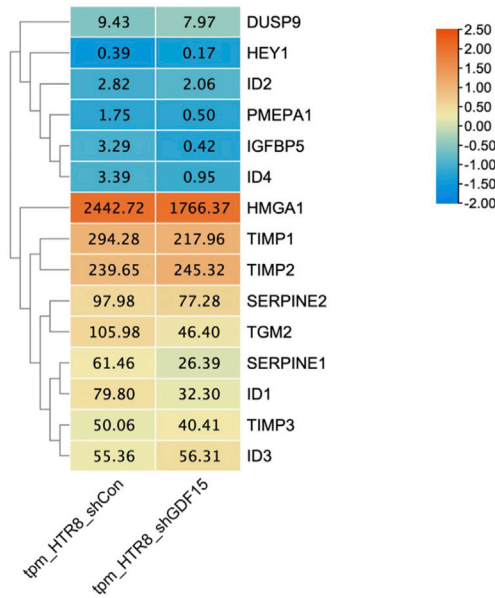
A Differential genes volcano map



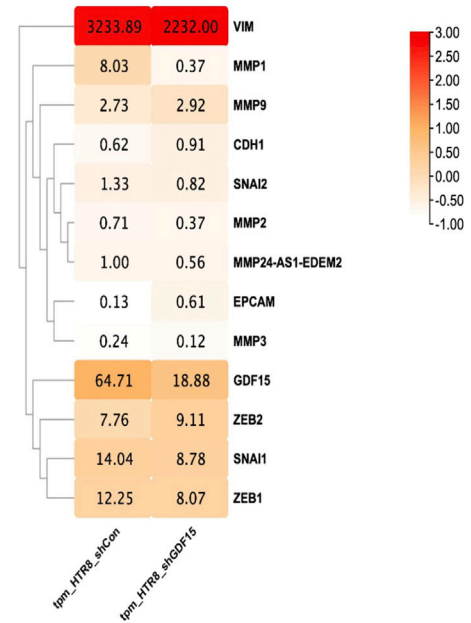
B KEGG pathway Enrichment bubbles pattern



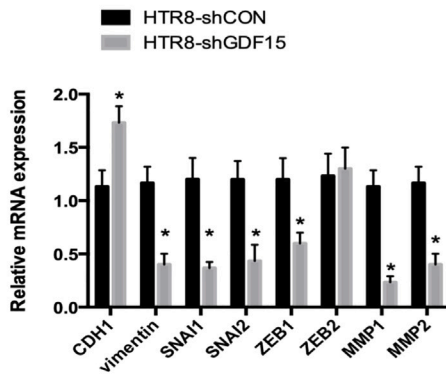
C



D



E



F

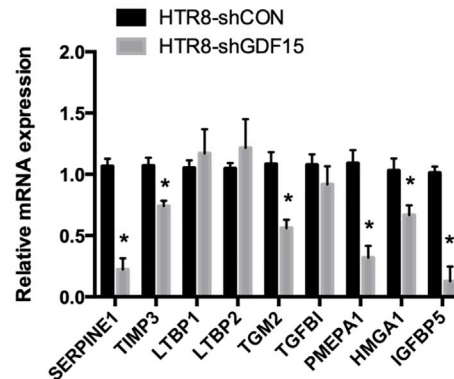


Figure 4. GDF15 activates the TGF- β pathway and regulates epithelial-mesenchymal transition (EMT)-related genes in HTR8/SVneo cells

(A) The volcano plot illustrates the differential expressed genes between GDF15-silencing cells and their control cells in HTR8/Svneo cell line. (B) The bubble chart presents the main enrichment pathways through GO analysis of differential gene expression. (C and D) (C) The TGF- β pathway related genes and epithelial-mesenchymal transition (EMT)-related genes (D) expressed differentially shown by heatmap visualization. (E and F) (E) The mRNA levels of genes related EMT and TGF- β pathway (F) were validated by real-time PCR assay. mRNA was quantified using qRT-PCR and normalized to b-actin. *, $p < 0.05$; **, $p < 0.01$; ***, $p < 0.001$ (unpaired two-tailed Student's *t* test). See also [Table S2](#) for further information.

GDF15 stimulates the TGF- β pathway by increasing of Smad1/5 phosphorylation

To determine whether GDF15 stimulates the TGF- β pathway through the transcription effect of Smad2/3 or Smad1/5, overexpression and silencing of GDF15 by lentivirus in HTR8/SVneo and JEG-3 cell lines were used in immunocytochemistry and western blotting. Immunocytochemistry analysis revealed that rhGDF15 treatment induced nucleus translocation of Smad5 but not Smad2 and Smad3 compared to those in PBS group in HTR8/SVneo cells ([Figure 5A](#)). Silencing GDF15 with lentivirus in JEG-3 cells also resulted in significantly lower Smad5 levels in the nucleus with no discernible difference of Smad2/3 compared to control cells ([Figure 5B](#)). Furthermore, western blotting assay showed that overexpression of GDF15 in both HTR8/SVneo and JEG-3 cells increased the protein levels of phosphorylated Smad1/5, VIMENTIN, and SNAI2 while decreasing the protein levels of E-CADHERIN compared to those in the respective control cells. Moreover, silencing GDF15 decreased the protein levels of phosphorylated Smad1/5, VIMENTIN, SNAI2 while increasing the protein levels of E-CADHERIN compared to the respective control cells. However, the protein levels of Smad5, Smad2, phosphorylated Smad2, Smad3 and phosphorylated Smad3 were not affected by the GDF15 change ([Figures 5C–5E](#)). Furthermore, Silencing Smad5 with shRNA attenuated the migration and invasion of HTR8/Svneo cells compared to the respective control cells by a transwell assay ([Figures 5F and 5G](#)). Western blotting revealed that VIMENTIN and SNAI2 protein levels were lower and E-CADHERIN levels were higher in HTR8/SVneo and JEG-3 Smad5-silencing cells than those in control cells ([Figures 5H and 5I](#)).

To assess GDF15's transcriptional effect on target genes, a dual luciferase reporter system was constructed in PGL3.0 vector with promoters of SNAI1/2, CDH1(E-CADHERIN), SERPINE1, TIMP3 and LTBP1, which contained the motifs of SBE (Smad binding element : GTCTGNCN) or GC-rich sites of SNAI1/2, SERPINE1, TIMP3, LTBP1 and E-box (CAGGTG) of CDH1 ([Figures 6A and 6B](#)). The luciferase activity of SNAI1/2, SERPINE1 and TIMP3 promoters was significantly higher while CDH1 promoter was significantly lower in GDF15-overexpression HTR8/SVneo cells than that in the respective control cells ([Figure 6C](#)). Moreover, the luciferase activity of SNAI1/2, SERPINE1 and TIMP3 promoter was significantly higher while CDH1 promoter was significantly lower in HTR8/SVneo GDF15-silencing cells than that in the respective control cells ([Figure 6D](#)). No change of luciferase activity of LTBP1 promoter was observed in the HTR8/SVneo GDF15-overexpression and silencing cells. All these results indicated that GDF15 accelerated the phosphorylation and nucleus translocation of Smad5 and regulating the target genes including SNAI1/2, CDH1, SERPINE1 and TIMP3.

Correlation analysis between the expression of GDF15 and Smad5, SNAI1 and SNAI2 in villus specimens

To validate the correlation between GDF15 expression and TGF- β signaling pathway related proteins in villus specimens, IHC was used to detect the expression of GDF15, Smad5, SNAI1 and SNAI2 in 18 villus from artificial abortion without pathological factors(Normal) 16 villus from spontaneous miscarriage (Miscarriage) ([Figure 7A](#)). Similar to GDF15 expression, the staining scores of Smad5, SNAI1 and SNAI2 in the villus of Miscarriage were significantly lower than those in the villus of Normal ([Figures 7B–7E](#)). Notably, a Pearson correlation analysis revealed that GDF15 expression was positively correlated with Smad5, SNAI1 and SNAI2 expression in 34 villus samples ($r^2 = 0.1377$, $p = 0.0307$; $r^2 = 0.1339$, $p = 0.0333$; $r^2 = 0.2317$, $p = 0.0039$ respectively, [Figures 7F–7H](#)). Therefore, those results indicated that GDF15 was linked to increased activity of the TGF- β /Smad5 signaling pathway in human trophoblast tissue.

DISCUSSION

Emerging evidence supports that TGF- β pathway plays a crucial role in trophoblast cell invasion and proliferation.^{2,10–12} However, the precise role of GDF15 in the induction of invasion of trophoblast during pregnancy remains to be elucidated. Our results shed new light on the role of GDF15 in trophoblast invasion. Trophoblast cells, particularly syncytiotrophoblast were the primary source of GDF15 in our immunocytochemistry assay ([Figure 1A](#)). Both HTR8/SVneo (trophoblast cell line) and JEG-3 (choriocarcinoma cell line) secreted GDF15 protein abundantly ([Figures S1A and S1B](#)). GDF15 is produced by decidual stromal cells and trophoblasts in other studies.^{13,14} The current study revealed that the expression of GDF15 in the trophoblast and serum significantly decreased in pregnant women with miscarriage. These results were consistent with the of Tong S's early findings that GDF15 was a predictor of first-trimester miscarriage.^{15,16} Furthermore, GDF15 is reduced in the trophoblast tissue of the abortion mouse model and GDF15 deficiency is associated with embryo resorption in mice. A lack of GDF15 expression predicted a poor pregnancy prognostic in both human and mice. GDF15 could be a biomarker for pregnancy outcome in women who have had spontaneous abortions in the past, and our data showed that lower GDF15 levels was associated with risk of adverse pregnancy outcome. GDF15 has been validated as a predictor of miscarriage in pregnant women. In summary, GDF15 is likely to be an important serum biomarker for guiding pregnancy progression and prognosis evaluation.

The invasive process of trophoblast following embryo implantation is essential for human placentation as well as pregnancy establishment and maintenance.¹⁷ Insufficient invasion of trophoblast cells of placenta into the maternal decidua directly results in a poor prognosis for pregnant patients.^{18,19} In this study, transwell assay showed that silencing GDF15 reduced invasive and migratory ability in HTR8/SVneo

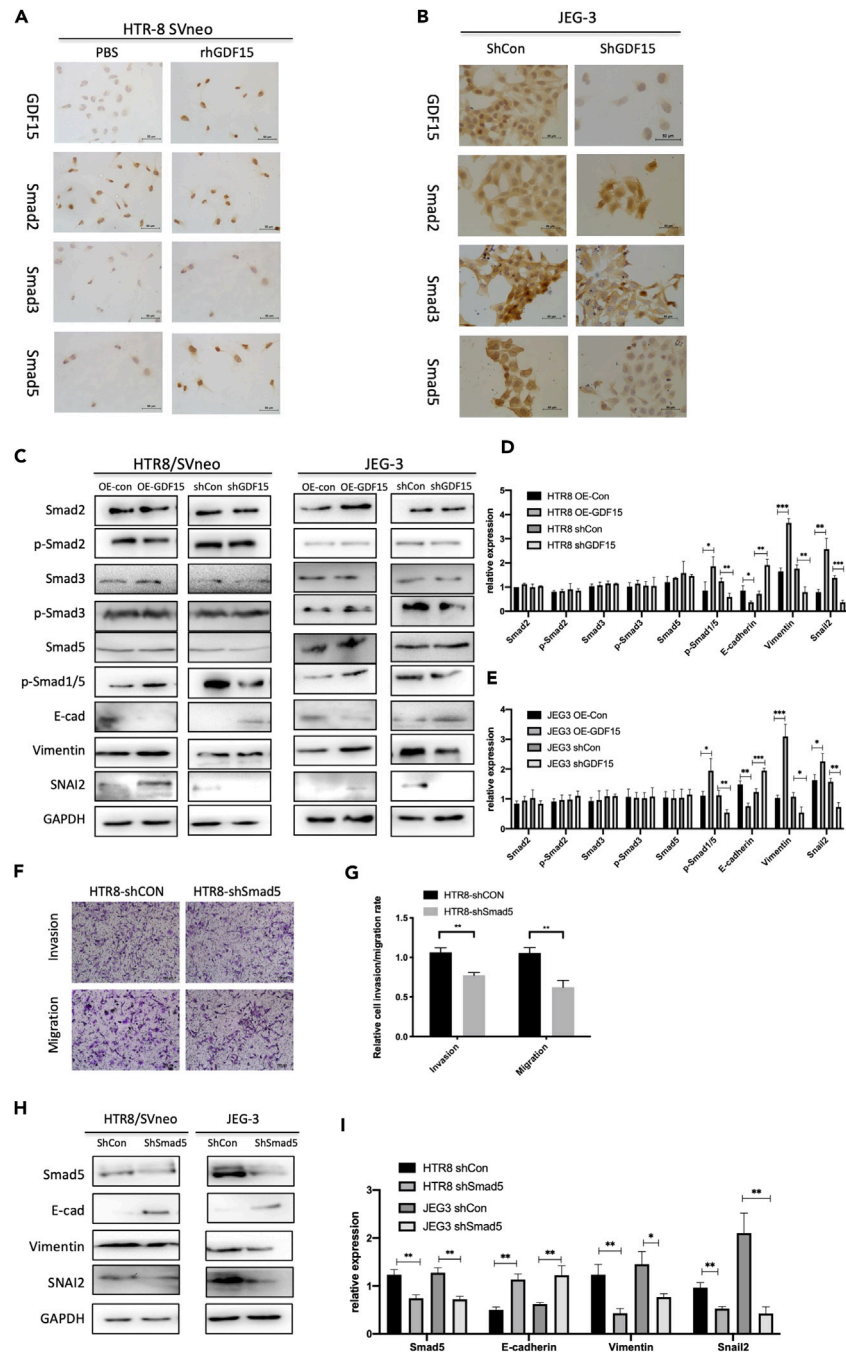


Figure 5. GDF15 activates the TGF- β pathway by increasing phosphorylation of Smad1/5

(A and B) (A) Immunocytochemistry for Smad2, Smad3 and Smad5 staining in HTR8/SVneo cell line after using PBS or rhGDF15 and JEG-3 cell line(B) after GDF15-silencing.

(C–E) (C) The expression of Smad2, *p*-Smad2, Smad3, *p*-Smad3, Smad5, *p*-Smad1/5, E-cadherin, Vimentin, SNAI2 and GAPDH protein in the GDF15-overexpression and GDF15 silencing HTR8/Sneo and JEG-3 cell lines and their control cell lines were detected by Western Blotting and the quantitative analysis were shown (D and E).

(F and G) (F) The invasive and migratory potential (G) of Smad5-silencing HTR8/Svneo cells and their control cells were analyzed by the transwell cell invasion and migration assays.

(H and I) (H) The expression of Smad5, E-cadherin, Vimentin, SNAI2 and GAPDH protein in the Smad5 silencing HTR8/Sneo and JEG-3 cell lines and their control cell lines were detected by Western Blotting and the quantitative analysis were shown and normalized to GAPDH (I). *, $p < 0.05$; **, $p < 0.01$; ***, $p < 0.001$ (unpaired two-tailed Student's *t* test).

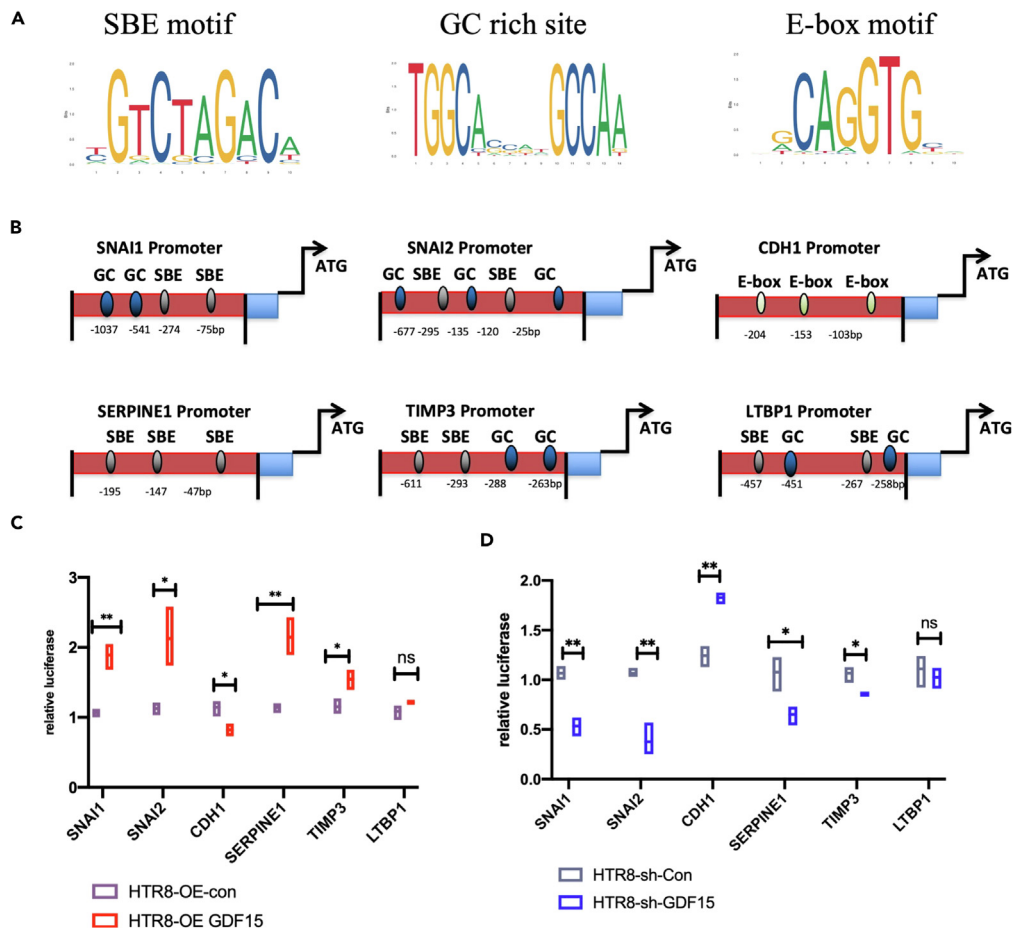


Figure 6. The alteration of GDF15 to the transcriptional regulation of Smad5-related genes

(A and B) The promoter structures of SNAI1/2, SERPINE1, TIMP3 and LTBP1 containing Smad-binding elements (SBE) or GC-rich motifs and CDH1 containing E-box were shown in the pattern diagram.

(C and D) The luciferase activity relative to Renilla control was measured in GDF15-overexpression and GDF15-silencing HTR8/Svneo cells and the respective control cells. $p < 0.05$; **, $p < 0.01$; ***, $p < 0.001$ (unpaired two-tailed Student's *t* test). See also Table S3 for further information.

and JEG-3 cell lines *in vitro*. Subsequently, we demonstrated that the addition of recombinant human GDF15 rescued cell invasion and migration *in vitro*. Using RNA sequencing and real-time PCR, we observed that trophoblast cells with GDF15 silencing expressed more E-CADHERIN and less Vimentin, SNAI1, SNAI2, ZEB1, MMP1 and MMP2. Silencing GDF15 expression had also altered TGF- β pathway related genes expression, such as SERPINE1, TIMP3, TGM2, PMEPA1, HMGA1, and IGFBP5. These data support that GDF15 may be involved in invasion and migration of HTR8/SVneo cells through TGF- β pathway signaling. In addition, previous research has found a link between GDF15 and invasion in other cancers.^{20–24}

Next, the molecular mechanism of GDF15 in trophoblast invasion was explored. There were several signaling pathways responsible in regulating trophoblast invasion, including PI3K/Akt/GSK3 β ,²⁵ Notch,²⁶ TGF- β ²⁷ and STAT3 pathways.²⁸ As previous stated, GDF15 is a member of TGF- β superfamily, the roles of other members such as TGF- β 1, BMPs, actins, and inhibins in trophoblast invasion have been discussed in detail in the review of Leung PCK.² Our study revealed overexpression of GDF15 had the opposite effect to that of silencing, promoting phosphorylation of Smad1/5 and production of Snail1/2 and Vimentin, while inhibiting the expression of E-cadherin. The immunocytochemistry assay indicated that rhGDF15 treatment increased Smad5 nucleus deposition, whereas silencing GDF15 has the opposite effect. No effect of phosphorylation of Smad2 and Smad3 was observed after ectopic expression or silencing of GDF15. It has been reported that Smad1/5 impedes E-cadherin transcription, which results in the stabilization of Snail.^{29,30} In our study, blockade of Smad5 by shRNA in HTR8/SVneo cells decreased invasion and migration, which was accompanied by Snail2 and Vimentin suppression. In summary, GDF15 promotes invasion and migration in trophoblast by increasing Snail1/2 and Vimentin expression through TGF- β /Smad1/5 pathway. Mad homolog domain 1 (MH1 domain) of Smad5 is essential for specific DNA binding, such as SBE or GC-rich motif.³¹ Consistently, overexpression and silencing of GDF15 in HTR8/SVneo cell altered the transcriptional activity of SNAI1/2, CDH1(E-Cadherin), SERPINE1 and TIMP3 via TGF- β /Smad1/5 pathway. Intriguingly, SERPINE1(PAI-1) and TIMP3 were reported to be transcriptionally activated by Smad2/3^{32–36} and SERPINE1 could

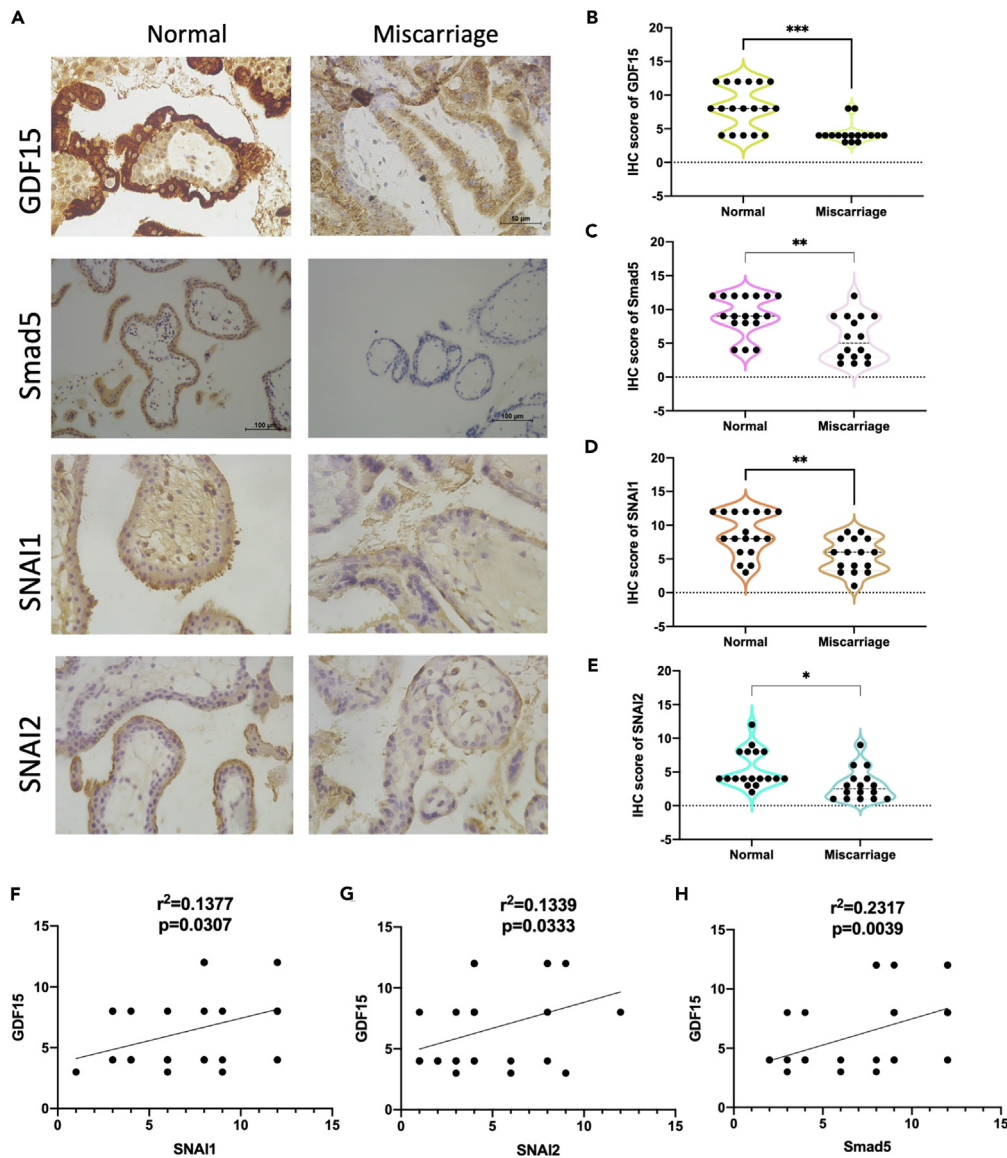


Figure 7. Correlation analysis between the expression of GDF15 and Smad5, SNAI1 and SNAI2 in villus specimens (A–E) (A) 18 normal villus and 16 miscarriage villus samples were analyzed by IHC and the representative expression of GDF15, Smad5, SNAI1 and SNAI2 is shown and staining score of each sample was quantified (B–E). (unpaired two-tailed Student’s t test). (F–H) Correlation of GDF15 and SNAI1, SNAI2 and Smad5 expression respectively was analyzed in the villus samples by Pearson Chi-Square test. $p < 0.05$; **, $p < 0.01$; ***, $p < 0.001$.

also be induced by TGF- β /Smad2/3 pathway.³⁷ Our study also suggests that SERPINE1 and TIMP3 are involved in GDF15-induced signal activation, implying that a crosstalk mechanism between GDF15 and non-Smad pathway exists. However, the exact mechanism has yet to be elucidated.

E-cadherin could enhance Smad1/5 phosphorylation in intervertebral discs,³⁸ whereas Smad5 also could downregulate E-cadherin expression and promote human glioma cells migration.^{39,40} Snail is a Smad-dependent transcriptional regulator,^{41,42} which was also verified to suppress the transcription level of E-cadherin.⁴³ Here, we reported that GDF15 promoted the Smad5 phosphorylation and nuclear translocation in trophoblast cells. Nuclear accumulation of Smad5 activated many transcriptional factors, including EMT-related genes. Expectedly, the levels of Vimentin and Snail2, two target genes of TGF- β pathway, were increased in response to GDF15 ectopic expression, and this effect can be reversed by Smad5 depletion. Previous research indicated that Vimentin and Snail2 acts as a powerfully inducer of invasion by repressing E-cadherin transcription in trophoblast.^{44–46} In our study, an increment of Vimentin and Snail2 followed by GDF15 might retard E-cadherin in the GDF15 overexpression cells or rhGDF15 treatment. Collectively, our study demonstrated that GDF15 enhances invasion and migration of trophoblast cells by regulation of Vimentin and Snail expression as well as E-cadherin transcription through TGF- β /Smad1/5 signaling.

In this study, we first demonstrated that GDF15 was a major enhancer of invasion in trophoblast cells using *in vitro* and *in vivo* assays as well as a group of pregnant women and animal models. Second, we showed that GDF15 could directly phosphorylate Smad1/5, activating TGF- β /Smad1/5 signaling and increasing Vimentin and Snail2 expression while decreasing E-cadherin. Accumulated nuclear Smad5 induced the transcription of Snail1/2, ZEB1/2, Vimentin, MMP1 and MMP2 as well as the reduction of E-cadherin, which consequently enhancing trophoblast cell migration and invasion. Finally, we discovered that GDF15 was positively correlated with Smad5 and Snail1/2 expression in clinical villus samples. In summary, these findings revealed that GDF15 stimulated invasion and migration in trophoblast. The critical signaling pathway involved in this process was identified, as were potential diagnostic and therapeutic targets in women with spontaneous miscarriage.

Limitations of the study

A potential limitation of this study is that we have not been able to present EVT in the IHC results, because we only found a small portion of EVT shown in our IHC results from villus samples. However, we have showed that GDF15 was abundantly expressed in both syncytiotrophoblast and EVT. The experiments were conducted to confirm the function of GDF15 in HTR8 cell line from EVT source.

STAR★METHODS

Detailed methods are provided in the online version of this paper and include the following:

- KEY RESOURCES TABLE
- RESOURCE AVAILABILITY
 - Lead contact
 - Materials availability
 - Data and code availability
- EXPERIMENTAL MODEL AND STUDY PARTICIPANT DETAILS
 - Human specimens
 - Cell lines
 - Spontaneous abortion animal model Construction and Transgene mice of GDF15
- METHOD DETAILS
 - The Human Cell Landscape (HCL) single-cell RNAseq database
 - Lentivirus infection
 - Immunohistochemistry and immunocytochemistry
 - Quantitative Polymerase Chain Reaction analysis and RNA sequence
 - Western blotting
 - ELISA assay
 - Transwell assays and scratch wound-healing assay
 - Luciferase reporter assay
- QUANTIFICATION AND STATISTICAL ANALYSIS

SUPPLEMENTAL INFORMATION

Supplemental information can be found online at <https://doi.org/10.1016/j.isci.2023.107902>.

ACKNOWLEDGMENTS

Funding Statement: Supported by grants received from the Fund for the National Natural Science Foundation of China (No. 81901497 and No.82003139).

AUTHOR CONTRIBUTIONS

S.L. contributed to study design and planning, conducting experiments, data analysis, and article preparation, and review. Y.T.Z. contributed to conducting experiments. W.F.L. contributed to data review and article preparation. P.S.Z. contributed to study design, data analysis, article preparation, and review.

DECLARATION OF INTERESTS

All authors declare that they have no conflict of interest in the article.

Received: January 30, 2023

Revised: May 4, 2023

Accepted: September 8, 2023

Published: September 13, 2023

REFERENCES

- Lee, C.Q., Gardner, L., Turco, M., Zhao, N., Murray, M.J., Coleman, N., Rossant, J., Hemberger, M., and Moffett, A. (2016). What Is Trophoblast? A Combination of Criteria Define Human First-Trimester Trophoblast. *Stem Cell Rep.*
- Li, Y., Yan, J., Chang, H.M., Chen, Z.J., and Leung, P.C.K. (2021). Roles of TGF- β Superfamily Proteins in Extravillous Trophoblast Invasion. *Trends Endocrinol. Metabol.* 32, 170–189. <https://doi.org/10.1016/j.tem.2020.12.005>.
- Cheng, J.C., Chang, H.M., and Leung, P.C.K. (2013). Transforming growth factor- β 1 inhibits trophoblast cell invasion by inducing Snail-mediated down-regulation of vascular endothelial-cadherin protein. *J. Biol. Chem.* 288, 33181–33192. <https://doi.org/10.1074/jbc.M113.488866>.
- Fang, L., Wang, Z., Wu, Z., Yan, Y., Gao, Y., Li, Y., Cheng, J.C., and Sun, Y.P. (2021). GDF-8 stimulates trophoblast cell invasion by inducing ALK5-SMAD2/3-mediated MMP2 expression. *Reproduction* 162, 331–338.
- Wu, Z., Fang, L., Yang, S., Gao, Y., Wang, Z., Meng, Q., Dang, X., Sun, Y.P., and Cheng, J.C. (2022). GDF-11 promotes human trophoblast cell invasion by increasing ID2-mediated MMP2 expression. *Cell Commun. Signal.* 20, 89. <https://doi.org/10.1186/s12964-022-00899-z>.
- Zhao, H.J., Klausen, C., Zhu, H., Chang, H.M., Li, Y., and Leung, P.C.K. (2020). Bone morphogenetic protein 2 promotes human trophoblast cell invasion and endothelial-like tube formation through ID1-mediated upregulation of IGF binding protein-3. *Faseb. J.* 34, 3151–3164. <https://doi.org/10.1096/fj.201902168RR>.
- Corre, J., Hébraud, B., and Bourin, P. (2013). Concise review: growth differentiation factor 15 in pathology: a clinical role? *Stem Cells Transl. Med.* 2, 946–952. <https://doi.org/10.5966/sctm.2013-0055>.
- Moore, A.G., Brown, D.A., Fairlie, W.D., Bauskin, A.R., Brown, P.K., Munier, M.L., Russell, P.K., Salamonsen, L.A., Wallace, E.M., and Breit, S.N. (2000). The transforming growth factor- β superfamily cytokine macrophage inhibitory cytokine-1 is present in high concentrations in the serum of pregnant women. *J. Clin. Endocrinol. Metab.* 85, 4781–4788. <https://doi.org/10.1210/jcem.85.12.7007>.
- Keelan, J.A., Wang, K., Chaiworapongsa, T., Romero, R., Mitchell, M.D., Sato, T.A., Brown, D.A., Fairlie, W.D., and Breit, S.N. (2003). Macrophage inhibitory cytokine 1 in fetal membranes and amniotic fluid from pregnancies with and without preterm labour and premature rupture of membranes. *Mol. Hum. Reprod.* 9, 535–540. <https://doi.org/10.1093/molehr/gag068>.
- Shih, J.C., Lin, H.H., Hsiao, A.C., Su, Y.T., Tsai, S., Chien, C.L., and Kung, H.N. (2019). Unveiling the role of microRNA-7 in linking TGF- β -Smad-mediated epithelial-mesenchymal transition with negative regulation of trophoblast invasion. *Faseb. J.* 33, 6281–6295. <https://doi.org/10.1096/fj.201801898RR>.
- Brooks, S.A., Martin, E., Smeester, L., Grace, M.R., Boggess, K., and Fry, R.C. (2016). miRNAs as common regulators of the transforming growth factor (TGF)- β pathway in the preeclamptic placenta and cadmium-treated trophoblasts: Links between the environment, the epigenome and preeclampsia. *Food Chem. Toxicol.* 98, 50–57. <https://doi.org/10.1016/j.fct.2016.06.023>.
- Koel, M., Vösa, U., Krjutskov, K., Einarsdottir, E., Kere, J., Tapanainen, J., Katayama, S., Ingerpuu, S., Jaks, V., Stenman, U.H., et al. (2017). Optimizing bone morphogenic protein 4-mediated human embryonic stem cell differentiation into trophoblast-like cells using fibroblast growth factor 2 and transforming growth factor- β /activin/nodal signalling inhibition. *Reprod. Biomed. Online* 35, 253–263. <https://doi.org/10.1016/j.rbmo.2017.06.003>.
- Segerer, S.E., Rieger, L., Kapp, M., Dombrowski, Y., Müller, N., Dietl, J., and Kämmerer, U. (2012). MIC-1 (a multifunctional modulator of dendritic cell phenotype and function) is produced by decidual stromal cells and trophoblasts. *Hum. Reprod.* 27, 200–209. <https://doi.org/10.1093/humrep/der358>.
- Turco, M.Y., Gardner, L., Kay, R.G., Hamilton, R.S., Prater, M., Hollinshead, M.S., McWhinnie, A., Esposito, L., Fernando, R., Skelton, H., et al. (2018). Trophoblast organoids as a model for maternal-fetal interactions during human placentation. *Nature* 564, 263–267. <https://doi.org/10.1038/s41586-018-0753-3>.
- Carbillon, L., Benzacken, B., and Uzan, M. (2004). MIC 1 concentration as a predictor of first-trimester miscarriage. *Lancet (London, England)* 363, 1238–1239. author reply 1239. [https://doi.org/10.1016/s0140-6736\(04\)15966-7](https://doi.org/10.1016/s0140-6736(04)15966-7).
- Tong, S., Marjono, B., Brown, D.A., Mulvey, S., Breit, S.N., Manuelpillai, U., and Wallace, E.M. (2004). Serum concentrations of macrophage inhibitory cytokine 1 (MIC 1) as a predictor of miscarriage. *Lancet (London, England)* 363, 129–130. [https://doi.org/10.1016/s0140-6736\(03\)15265-8](https://doi.org/10.1016/s0140-6736(03)15265-8).
- Velicky, P., Knöfler, M., and Pollheimer, J. (2016). Function and control of human invasive trophoblast subtypes: Intrinsic vs. maternal control. *Cell Adhes. Migrat.* 10, 154–162. <https://doi.org/10.1080/19336918.2015.1089376>.
- Park, J.Y., Mani, S., Clair, G., Olson, H.M., Paurus, V.L., Ansong, C.K., Blundell, C., Young, R., Kanter, J., Gordon, S., et al. (2022). A microphysiological model of human trophoblast invasion during implantation. *Nat. Commun.* 13, 1252. <https://doi.org/10.1038/s41467-022-28663-4>.
- Illsley, N.P., DaSilva-Arnold, S.C., Zamudio, S., Alvarez, M., and Al-Khan, A. (2020). Trophoblast invasion: Lessons from abnormally invasive placenta (placenta accreta). *Placenta* 102, 61–66. <https://doi.org/10.1016/j.placenta.2020.01.004>.
- Dong, G., Huang, X., Jiang, S., Ni, L., Ma, L., Zhu, C., and Chen, S. (2020). SCAP Mediated GDF15-Induced Invasion and EMT of Esophageal Cancer. *Front. Oncol.* 10, 564785. <https://doi.org/10.3389/fonc.2020.564785>.
- Li, C., Wang, J., Kong, J., Tang, J., Wu, Y., Xu, E., Zhang, H., and Lai, M. (2016). GDF15 promotes EMT and metastasis in colorectal cancer. *Oncotarget* 7, 860–872. <https://doi.org/10.18632/oncotarget.6205>.
- Ding, Y., Hao, K., Li, Z., Ma, R., Zhou, Y., Zhou, Z., Wei, M., Liao, Y., Dai, Y., Yang, Y., et al. (2020). c-Fos separation from Lamin A/C by GDF15 promotes colon cancer invasion and metastasis in inflammatory microenvironment. *J. Cell. Physiol.* 235, 4407–4421. <https://doi.org/10.1002/jcp.29317>.
- Jin, Y., Jung, S.N., Lim, M.A., Oh, C., Piao, Y., Kim, H.J., Liu, L., Kang, Y.E., Chang, J.W., Won, H.R., et al. (2021). Transcriptional Regulation of GDF15 by EGR1 Promotes Head and Neck Cancer Progression through a Positive Feedback Loop. *Int. J. Mol. Sci.* 22, 11151. <https://doi.org/10.3390/ijms222011151>.
- Jiang, G., Liu, C.T., and Zhang, W.D. (2018). IL-17A and GDF15 are able to induce epithelial-mesenchymal transition of lung epithelial cells in response to cigarette smoke. *Exp. Ther. Med.* 16, 12–20. <https://doi.org/10.3892/etm.2018.6145>.
- Wang, J., Ding, J., Zhang, S., Chen, X., Yan, S., Zhang, Y., and Yin, T. (2021). Decreased USP2a Expression Inhibits Trophoblast Invasion and Associates With Recurrent Miscarriage. *Front. Immunol.* 12, 717370. <https://doi.org/10.3389/fimmu.2021.717370>.
- Luo, Q., Zhang, W., Liu, X., Zheng, Y., Gao, H., Zhao, Y., and Zou, L. (2020). Delta-Like 4-Notch signaling regulates trophoblast migration and invasion by targeting EphrinB2. *Biochem. Biophys. Res. Commun.* 527, 915–921. <https://doi.org/10.1016/j.bbrc.2020.05.032>.
- AbdelHafez, F., Klausen, C., Zhu, H., and Leung, P.C.K. (2022). Myostatin increases human trophoblast cell invasion by upregulating N-cadherin via SMAD2/3-SMAD4 signaling. *Biol. Reprod.* 106, 1267–1277. <https://doi.org/10.1093/biolre/iob238>.
- Zhang, W., Yang, M., Yu, L., Hu, Y., Deng, Y., Liu, Y., Xiao, S., and Ding, Y. (2020). Long Non-coding RNA Lnc-DC in Dendritic Cells Regulates Trophoblast Invasion via P-STAT3-Mediated TIMP/MMP Expression. *Am. J. Reprod. Immunol.* 83, e13239. <https://doi.org/10.1111/aji.13239>.
- Yao, Y., Chen, R., Wang, G., Zhang, Y., and Liu, F. (2019). Exosomes derived from mesenchymal stem cells reverse EMT via TGF- β /Smad pathway and promote repair of damaged endometrium. *Stem Cell Res. Ther.* 10, 225. <https://doi.org/10.1186/s13287-019-1332-8>.
- Kee, J.Y., Han, Y.H., Mun, J.G., Park, S.H., Jeon, H.D., and Hong, S.H. (2019). Effect of Korean Red Ginseng extract on colorectal lung metastasis through inhibiting the epithelial-mesenchymal transition via transforming growth factor- β /Smad-signaling-mediated Snail/E-cadherin expression. *J. Ginseng Res.* 43, 68–76. <https://doi.org/10.1016/j.jgr.2017.08.007>.
- Chai, N., Li, W.X., Wang, J., Wang, Z.X., Yang, S.M., and Wu, J.W. (2017). Structural basis for the Smad5 MH1 domain to recognize different DNA sequences. *Nucleic Acids Res.* 45, 6255–6257.
- Samarakoon, R., Overstreet, J.M., Higgins, S.P., and Higgins, P.J. (2012). TGF- β 1 \rightarrow SMAD/p53/USF2 \rightarrow PAI-1 transcriptional axis in ureteral obstruction-induced renal fibrosis. *Cell Tissue Res.* 347, 117–128. <https://doi.org/10.1007/s00441-011-1181-y>.
- Vayalil, P.K., Iles, K.E., Choi, J., Yi, A.K., Postlethwait, E.M., and Liu, R.M. (2007). Glutathione suppresses TGF-beta-induced PAI-1 expression by inhibiting p38 and JNK MAPK and the binding of AP-1, SP-1, and Smad to the PAI-1 promoter. *Am. J. Physiol.*

- Lung Cell Mol. Physiol. 293, L1281–L1292. <https://doi.org/10.1152/ajplung.00128>.
34. Zhou, Q., Zheng, X., Chen, L., Xu, B., Yang, X., Jiang, J., and Wu, C. (2016). Smad2/3/4 Pathway Contributes to TGF- β -Induced MiRNA-181b Expression to Promote Gastric Cancer Metastasis by Targeting Timp3. *Cell. Physiol. Biochem.* 39, 453–466. <https://doi.org/10.1159/000445638>.
 35. Liang, J., Chen, M., Hughes, D., Chumanevich, A.A., Altiglia, S., Kaza, V., Lim, C.U., Kiaris, H., Myhre, K., Pena, M.M., et al. (2018). CDK8 Selectively Promotes the Growth of Colon Cancer Metastases in the Liver by Regulating Gene Expression of TIMP3 and Matrix Metalloproteinases. *Cancer Res.* 78, 6594–6606. <https://doi.org/10.1158/0008-5472.Can-18-1583>.
 36. Wang, B., Hsu, S.H., Majumder, S., Kutay, H., Huang, W., Jacob, S.T., and Ghoshal, K. (2010). TGF β -mediated upregulation of hepatic miR-181b promotes hepatocarcinogenesis by targeting TIMP3. *Oncogene* 29, 1787–1797. <https://doi.org/10.1038/onc.2009.468>.
 37. Cheng, A., Gustafson, A.R., Schaner Tooley, C.E., and Zhang, M. (2016). BMP-9 dependent pathways required for the chondrogenic differentiation of pluripotent stem cells. *Differentiation* 92, 298–305. <https://doi.org/10.1016/j.diff.2016.03.005>.
 38. Wang, Z., Kim, S., Hutton, W., and Yoon, S. (2012). E-cadherin upregulates expression of matrix macromolecules aggrecan and collagen II in the intervertebral disc cells through activation of the intracellular BMP-Smad1/5 pathway. *J. Orthop. Res.* 30, 1746–1752. <https://doi.org/10.1002/jor.22153>.
 39. Chang, S.F., Yang, W.H., Cheng, C.Y., Luo, S.J., and Wang, T.C. (2021). γ -secretase inhibitors, DAPT and RO4929097, promote the migration of Human Glioma Cells via Smad5-downregulated E-cadherin Expression. *Int. J. Med. Sci.* 18, 2551–2560. <https://doi.org/10.7150/ijms.50484>.
 40. Zhao, X., Sun, Q., Dou, C., Chen, Q., and Liu, B. (2019). BMP4 inhibits glioblastoma invasion by promoting E-cadherin and claudin expression. *Front. Biosci.* 24, 1060–1070. <https://doi.org/10.2741/4768>.
 41. Savary, K., Caglayan, D., Caja, L., Tzavlaki, K., Bin Nayeem, S., Bergström, T., Jiang, Y., Uhrbom, L., Forsberg-Nilsson, K., Westermark, B., et al. (2013). Snail depletes the tumorigenic potential of glioblastoma. *Oncogene* 32, 5409–5420. <https://doi.org/10.1038/onc.2013.67>.
 42. Chandran Latha, K., Sreekumar, A., Beena, V., S S, B., Lakkappa, R., Kalyani, R., Nair, R., Kalpana, S., Kartha, C., and Surendran, S. (2021). Shear Stress Alterations Activate BMP4/pSMAD5 Signaling and Induce Endothelial Mesenchymal Transition in Varicose Veins. *Cells* 10. <https://doi.org/10.3390/cells10123563>.
 43. Gao, J., Liu, R., Feng, D., Huang, W., Huo, M., Zhang, J., Leng, S., Yang, Y., Yang, T., Yin, X., et al. (2021). Snail/PRMT5/NuRD complex contributes to DNA hypermethylation in cervical cancer by TET1 inhibition. *Cell Death Differ.* 28, 2818–2836. <https://doi.org/10.1038/s41418-021-00786-z>.
 44. Wu, D., Shi, L., Chen, X., Cen, H., and Mao, D. (2020). β -TrCP suppresses the migration and invasion of trophoblast cells in preeclampsia by down-regulating Snail. *Exp. Cell Res.* 395, 112230. <https://doi.org/10.1016/j.yexcr.2020.112230>.
 45. Li, Y., Klausen, C., Zhu, H., and Leung, P.C.K. (2015). Activin A Increases Human Trophoblast Invasion by Inducing SNAIL-Mediated MMP2 Up-Regulation Through ALK4. *J. Clin. Endocrinol. Metab.* 100, E1415–E1427. <https://doi.org/10.1210/jc.2015-2134>.
 46. Zou, Y., Li, S., Wu, D., Xu, Y., Wang, S., Jiang, Y., Liu, F., Jiang, Z., Qu, H., Yu, X., et al. (2019). Resveratrol promotes trophoblast invasion in pre-eclampsia by inducing epithelial-mesenchymal transition. *J. Cell Mol. Med.* 23, 2702–2710. <https://doi.org/10.1111/jcmm.14175>.

STAR★METHODS

KEY RESOURCES TABLE

REAGENT or RESOURCE	SOURCE	IDENTIFIER
Antibodies		
Rabbit polyclonal antibody to GDF15	Santa Cruze	sc-66904
Rabbit polyclonal antibody to Smad2	Cell Signaling	#5339
Rabbit polyclonal antibody to phospho Smad2(Ser465/Ser467)	Cell Signaling	#18338
Rabbit polyclonal antibody to Smad3	Cell Signaling	#9532
Rabbit polyclonal antibody to phospho Smad3 (Ser423/425)	Cell Signaling	#9520
Rabbit polyclonal antibody to Smad5	Cell Signaling	#12534
Rabbit polyclonal antibody to phospho Smad5(Ser463/465)	Cell Signaling	#9516
Rabbit polyclonal antibody to SNAI1	Cell Signaling	#3819
Rabbit polyclonal antibody to SNAI2	Cell Signaling	#9585
Mouse monoclonal antibody VIMENTIN	Santa Cruze	sc-6260
Mouse monoclonal antibody E-CADHERIN	Santa Cruze	sc-8426
Mouse monoclonal antibody GAPDH	Santa Cruze	sc-47724
Bacterial and virus strains		
shGDF15 lentivirus	GeneChem biology company	N/A
shSmad5 vetors	GeneChem biology company	N/A
Chemicals, peptides, and recombinant proteins		
rhGDF15	Raybiotech	228-12036-2
TGF- β 1	MCE	HY-P70543
penicillin	Invitrogen	15070063
streptomycin	Invitrogen	15070064
Puromycin	Sigma	P8833
Lipofetamine 2000	Invitrogen	11668019
Matrigel	BD	354234
Critical commercial assays		
human GDF15 ELISA kit	R&D system	#DGD150
Dual-luciferase Assay Kit	Promega	E1960
RNAiso	TaKaRa	9108
PrimeScript RT Reagent Kit	TaKaRa	RR037A
SYRB-Green fluorescence signal detection assay	TaKaRa	RR420L
Experimental models: Cell lines		
HTR8/SVneo cells	ATCC	CRL-3271
JAR cells	ATCC	HTB-36
JEG-3 cells	ATCC	HTB -144
Experimental models: Organisms/strains		
CBA/J	Charles river	N/A
BALB/c	Charles river	N/A
C57BL/6N GDF15+/-	Cyagen	N/A

(Continued on next page)

Continued

REAGENT or RESOURCE	SOURCE	IDENTIFIER
Oligonucleotides		
Primers for real time RCR, see Table S2	This paper	N/A
Primers for LUC detection, see Table S3	This paper	N/A
Recombinant DNA		
pIRES2-AcGFP1-Neo	This paper	N/A
pIRES2-AcGFP1-Neo-GDF15	This paper	N/A
Software and algorithms		
Prism Graphpad 7.0	GraphPad Software	https://www.graphpad.com/
ImageJ	Schneider et al. ⁷	https://ImageJ.nih.gov/ij/

RESOURCE AVAILABILITY

Lead contact

Further information and requests for resources and reagents should be directed to and will be fulfilled by the Lead Contact, Shan Li (lishan2.0521@stu.xjtu.edu.cn). Corresponding Email: zpsheing@mail.xjtu.edu.cn and lishan2.0521@stu.xjtu.edu.cn.

Materials availability

GDF15 CRISPR/CAS9-based knockout C57 mice are available upon request.

Data and code availability

- Data reported in this paper will be shared by the [lead contact](#) upon request.
- This paper does not report original code.
- Any additional information required to reanalyze the data reported in this paper is available from the [lead contact](#) upon request.

EXPERIMENTAL MODEL AND STUDY PARTICIPANT DETAILS

Human specimens

A total of 18 villus samples from women who underwent induced abortions without medical reasons and 16 villus samples from women who experienced spontaneous abortion between 8 and 9 weeks of gestation were collected from the First Affiliated Hospital of Xi'an Jiaotong University from 2014 to 2016. A total of 79 serums from pregnant women had a live birth and 83 serums from pregnant women who spontaneously aborted were collected from 4 to 10 gestational weeks respectively. The study was approved by the institutional review board named as Ethics Committee of Medical School of Xi'an Jiaotong University in Shannxi, China. All the participants were informed the consent before collection.

Cell lines

The human trophoblast cell lines HTR8/SVneo, JAR and JEG-3 was purchased from ATCC. The HTR8/SVneo cells were cultured in Dulbecco's modified Eagle's medium (DMEM)/F-12 (supplemented with 10% fetal bovine serum (FBS)(BI) and 100units/ml of penicillin and streptomycin (Invitrogen, Waltham, MA United States). JAR and JEG-3 was cultured in DMEM with 10%FBS at 37 in a 5% CO2 atmosphere. The medium was replaced every 2 to 3 days. Extrinsic rhGDF15 (Raybiotech, Norcross, GA, United States, 50ng/ml) and TGF-β1 (MCE, United States, 10ng/ml) was purchased from recombinant proteins.

Spontaneous abortion animal model Construction and Transgene mice of GDF15

Five CBA/J female mice and five BALB/c male mice were mated to constructed normal pregnancy model, five CBA/J female mice and five DBA/2 male mice were mated to constructed spontaneous abortion model[49]. The animals were obtained from (Vital River Laboratory Animal Technology Co., Ltd., Beijing, China). C57BL/6N wild type (GDF15+/+), GDF15 heterozygote (GDF15+/-) and GDF15 homozygote (GDF15-/-) were obtained from Cyagen (Guangzhou, China). At day 12.5, all female mice were sacrificed to examine embryo resorption. All experimental mice used were specific-pathogen free (SPF). This study was approved by the Institute of Animal Committee at the Medical College of Xi'an Jiaotong University. The male mice cohabited with the female ones (1:2) to test the quantity and the embryo resorption rate of their offspring. embryo resorption rate= absorbed fetus/ (absorbed fetus+ normal fetus) .

METHOD DETAILS

The Human Cell Landscape (HCL) single-cell RNAseq database

All data was achieved from the website(bis.zju.edu.cn/HCL/). Single cell gene expression and cluster analysis were conducted in single cell level in the landscape.

Lentivirus infection

Overexpression plasmid and small RNA interference (siRNA) encapsulated by stable knockdown (shRNA) lentivirus were obtained from GeneChem biology company (Shanghai, China). Puromycin (Invitrogen, United States, 5 μ g/ml) was used to selected stable infected cells. RT-qPCR and/or Western blotting assays were applied to verified the infection efficiency.

Immunohistochemistry and immunocytochemistry

The immunohistochemical (IHC) and immunocytochemistry assays were performed as previously described[47]. The primary antibodies were GDF15(1:100, Santa Cruze, USA), Smad2(1:100, CST, USA), Smad3(1:100, CST, USA), Smad5(1:100, WanLei, China), SNAI1(1:100, Santa Cruze, USA), SNAI2 (1:100, CST, USA), VIMENTIN (1:100, Santa Cruze, USA) and E-CADHERIN (1:100, Santa Cruze, USA). The GDF15 staining was divided into groups based on the positive percentage and staining density. Positive percentage scores were categorized into five grades:0-5% (0), 6-25% (1), 26-50% (2), 51-75% (3) and 76-100% (4). The staining intensity was graded as follows: unstained (0), weak (1), moderate (2), strong (3). By multiplying the "staining intensity grade" by the "positive percentage score", the immune-reactivity score (IRS) was calculated. The standard is as follows: ≤ 2 (negative) , 3-9 (week positive), 9-12 (strong positive).

Quantitative Polymerase Chain Reaction analysis and RNA sequence

RNAiso (TaKaRa, Osaka, Japan) was used to isolate total RNA and the PrimeScript RT Reagent Kit (TaKaRa, Osaka, Japan) was used to synthesize cDNA. SYBR-Green fluorescence signal detection assay (TaKaRa, Osaka, Japan) was conducted for real-time RCR. The gene ACTB was used to normalize the results quantified by the 2- $\Delta\Delta$ CT method on an Gentier 96E instrument (TianLong, China). The RNA of HTR8/SVneo-shCon and HTR8/SVneo-shGDF15 was used to conduct RNA-seq in the BGISEQ-500 platform. The data was analyzed using the NOISeq method with the threshold log₂ fold-change >2.

Western blotting

Western blotting analyses were performed as previously described using 50 μ g lysate from fresh tissue and cells[48]. Protein was visualized using enhanced enhanced chemiluminescence detection system (Tanon 5100). The primary antibodies were GDF15(1:1000, Santa Cruze, USA), Smad2(1:500, CST, USA), phosphorylated Smad2 (Ser465/Ser467, 1:500, CST, USA), Smad3(1:500, CST, USA), phosphorylated Smad3 (Ser423/425, 1:500, CST, USA), Smad5 (1:1000, WanLei, China), phosphorylated Smad1/5(Ser463/465, 1:1000, CST, USA), VIMENTIN (1:1000, Santa Cruze, USA), E-CADHERIN (1:500, Santa Cruze, USA), SNAI2 (1:500, CST, USA) , GAPDH(1:10000, Proteintech, China).

ELISA assay

GDF15 levels in human serum were determined using a human GDF15 ELISA kit (#DGD150, R&D system, Minneapolis, MN, USA). The serum from peripheral blood was collected and diluted 10 times. The procedures were carried out in accordance with the manufacturer's instructions for the commercial kit. The optical density of each well was measured at 450nm and the concentrations of each sample were calculated using standard curves.

Transwell assays and scratch wound-healing assay

To assess trophoblast cells invasion, Matrigel (40 μ l, 1:8 dilution rate; Sigma, St Louis, MO) precoated transwell inserts (Corning, Cambridge, MA) with 8.0 nm diameter were used. Matrigel-free precoated transwell inserts were used to evaluate trophoblast cell migration. For the scratch wound assay, HTR8/Svneo cells/well (1×10^6) were seeded into a 6-well plate and incubated until confluent. A tip was used to scratch each well and the FBS-free medium was used to wash the detached cells at 0 hour and 48 hours respectively.

Luciferase reporter assay

For the luciferase reporter plasmid, fragments of the SNAI1/2, CDH1, SERPINE1, TIMP3 and LTBP1 promoters were cloned into pGL3.0 Basic Vector (Promega , Madison , WI , USA). The primers were listed in the [Table S3](#). GDF15-modified cells were seeded into 24-well-plates and Lipofetamine 2000 (Invitrogen) was used to co-transfected with reconstructed plasmids and pRL-TK plasmids. Dual-luciferase Assay Kit (Promega , Madison , WI , USA) was used to detect luciferase activities by luminometer (Promega).

QUANTIFICATION AND STATISTICAL ANALYSIS

Each sample was applied at least three times. To compare the significance of difference, data was calculated using the Student's t-test or the Chi-square test. The correlation was investigated using Pearson linear-regression analysis. Statistical analyses were performed with Prism Graphpad 7.0 (GraphPad Software, San Diego, California USA, www.graphpad.com). P value less than 0.05 were deemed statistically significant.